JCI The Journal of Clinical Investigation

α1G-dependent T-type Ca^{2+} current antagonizes cardiac hypertrophy through a NOS3-dependent mechanism in mice

Hiroyuki Nakayama, … , Arnold Schwartz, Jeffery D. Molkentin

J Clin Invest. 2009;119(12):3787-3796. https://doi.org/10.1172/JCI39724.

Research Article **Cardiology**

In noncontractile cells, increases in intracellular Ca^{2+} concentration serve as a second messenger to signal proliferation, differentiation, metabolism, motility, and cell death. Many of these Ca^{2+}-dependent regulatory processes operate in cardiomyocytes, although it remains unclear how Ca^{2+} serves as a second messenger given the high Ca^{2+} concentrations that control contraction. T-type Ca^{2+} channels are reexpressed in adult ventricular myocytes during pathologic hypertrophy, although their physiologic function remains unknown. Here we generated cardiac-specific transgenic mice with inducible expression of α1G, which generates $Ca_v3.1$ current, to investigate whether this type of Ca^{2+} influx mechanism regulates the cardiac hypertrophic response. Unexpectedly, α1G transgenic mice showed no cardiac pathology despite large increases in Ca^{2+} influx, and they were even partially resistant to pressure overload–, isoproterenol-, and exercise-induced cardiac hypertrophy. Conversely, $\alpha 1G^{-/-}$ mice displayed enhanced hypertrophic responses following pressure overload or isoproterenol infusion. Enhanced hypertrophy and disease in $\alpha 1G^{-/-}$ mice was rescued with the α1G transgene, demonstrating a myocyte-autonomous requirement of *α1G* for protection. Mechanistically, α1G interacted with NOS3, which augmented cGMP-dependent protein kinase type I activity in α1G transgenic hearts after pressure overload. Further, the anti-hypertrophic effect of α1G overexpression was abrogated by a NOS3 inhibitor and by crossing the mice onto the $Nos3^{-/-}$ background. Thus, cardiac α1G reexpression and its associated pool of T-type Ca^{2+} antagonize cardiac hypertrophy through a NOS3-dependent signaling mechanism. […]

α1G-dependent T-type Ca^{2+} current antagonizes cardiac hypertrophy through a NOS3-dependent mechanism in mice

Hiroyuki Nakayama,[1] Ilona Bodi,[2] Robert N. Correll,[1] Xiongwen Chen,[3] John Lorenz,[4] Steven R. Houser,[3] Jeffrey Robbins,[1] Arnold Schwartz,[2] and Jeffery D. Molkentin[1]

[1]Department of Pediatrics, University of Cincinnati, Division of Molecular Cardiovascular Biology, Howard Hughes Medical Institute, Children's Hospital Medical Center, Cincinnati, Ohio, USA. [2]Institute of Molecular Pharmacology and Biophysics, University of Cincinnati, Cincinnati, Ohio, USA. [3]Department of Physiology, Temple University School of Medicine, Philadelphia, Pennsylvania, USA. [4]Department of Systems Biology, University of Cincinnati, Cincinnati, Ohio, USA.

In noncontractile cells, increases in intracellular Ca^{2+} concentration serve as a second messenger to signal proliferation, differentiation, metabolism, motility, and cell death. Many of these Ca^{2+}-dependent regulatory processes operate in cardiomyocytes, although it remains unclear how Ca^{2+} serves as a second messenger given the high Ca^{2+} concentrations that control contraction. T-type Ca^{2+} channels are reexpressed in adult ventricular myocytes during pathologic hypertrophy, although their physiologic function remains unknown. Here we generated cardiac-specific transgenic mice with inducible expression of α1G, which generates $Ca_v3.1$ current, to investigate whether this type of Ca^{2+} influx mechanism regulates the cardiac hypertrophic response. Unexpectedly, α1G transgenic mice showed no cardiac pathology despite large increases in Ca^{2+} influx, and they were even partially resistant to pressure overload–, isoproterenol-, and exercise-induced cardiac hypertrophy. Conversely, *α1G*$^{-/-}$ mice displayed enhanced hypertrophic responses following pressure overload or isoproterenol infusion. Enhanced hypertrophy and disease in *α1G*$^{-/-}$ mice was rescued with the α1G transgene, demonstrating a myocyte-autonomous requirement of *α1G* for protection. Mechanistically, α1G interacted with NOS3, which augmented cGMP-dependent protein kinase type I activity in α1G transgenic hearts after pressure overload. Further, the anti-hypertrophic effect of α1G overexpression was abrogated by a NOS3 inhibitor and by crossing the mice onto the *Nos3*$^{-/-}$ background. Thus, cardiac α1G reexpression and its associated pool of T-type Ca^{2+} antagonize cardiac hypertrophy through a NOS3-dependent signaling mechanism.

Introduction

Cardiac hypertrophy occurs in response to physiologic stimuli such as exercise and in response to pathophysiologic stimuli such as hypertension, ischemic heart disease, valvular insufficiency, infectious agents, or mutations in sarcomeric genes (1). Pathologic hypertrophy temporarily maintains output, although prolongation of the hypertrophic state can predispose to arrhythmia and sudden death, as well as dilated cardiomyopathy and heart failure (2, 3). Ca^{2+} is one potential second messenger hypothesized to initiate cardiac hypertrophy, although it remains unclear how Ca^{2+} is sensed by reactive intracellular signaling pathways in the heart given the dynamic changes in total cytosolic Ca^{2+} that underlie excitation-contraction coupling (ECC) (4). Specialized pools of Ca^{2+} that are location specific or buffered from cytosolic Ca^{2+} fluxing could account for the regulation of Ca^{2+}-sensitive signaling proteins, such as calcineurin, protein kinase C, or Ca^{2+}/calmodulin-activated protein kinase II (CaMKII). For example, CaMKII is activated in cardiomyocytes by a perinuclear Ca^{2+} pool due to inositol triphosphate receptor ($InsP_3R$) activity (5). The voltage-gated L-type Ca^{2+} channel (LTCC), which underlies Ca^{2+}-induced Ca^{2+} release and contraction, may also localize to specialized lipid raft–containing membrane domains that serve as signal transduction organizing centers (6). Increased Ca^{2+} influx due to overexpression of the α1C pore-forming subunit or the β2a accessory subunit of the LTCC in the hearts of transgenic mice induces profound disease, indicating that increased Ca^{2+} influx can mediate pathologic cardiac hypertrophy (7, 8). We also recently showed that plasma membrane Ca^{2+} ATPase (PMCA) overexpression in the hearts of transgenic mice, which presumably removes Ca^{2+} near the sarcolemma, antagonized cardiac hypertrophy and calcineurin activation (9).

Fetal and early neonatal myocytes express T-type Ca^{2+} channels (TTCCs), although this expression is lost with maturation of the myocardium, so that the adult heart only shows TTCC current in myocytes of the conducting system (10). TTCCs have a relatively low conductance and operate at more negative potentials, and they are not thought to meaningfully participate in ECC in the heart when reexpressed (10). TTCC current results from the function of 3 distinct α subunits encoded by 3 separate genes, *α1G* ($Ca_v3.1$), *α1H* ($Ca_v3.2$), and *α1I* ($Ca_v3.3$) (10). TTCC currents are dramatically upregulated in ventricular myocytes from hypertrophied adult cat hearts, suggesting that TTCC genes are part of the fetal gene program that reemerges during adult pathology (11). Reexpression of T-type current has also been reported in pressure-overloaded rat and mouse hearts, in many different models of heart failure, and after myocardial infarction injury (12–16). More recently, reinduction of T-type current in the failing rat heart was shown to be dependent on endothelin-1 signaling (17). Reexpression of T-type current in the diseased myocardium conducts additional Ca^{2+} influx during the action potential, although the function of this Ca^{2+} influx remains unknown. One recent hypothesis is that TTCC current reexpression may have a signaling function in the

Conflict of interest: The authors have declared that no conflict of interest exists.
Citation for this article: *J. Clin. Invest.* **119**:3787–3796 (2009). doi:10.1172/JCI39724.

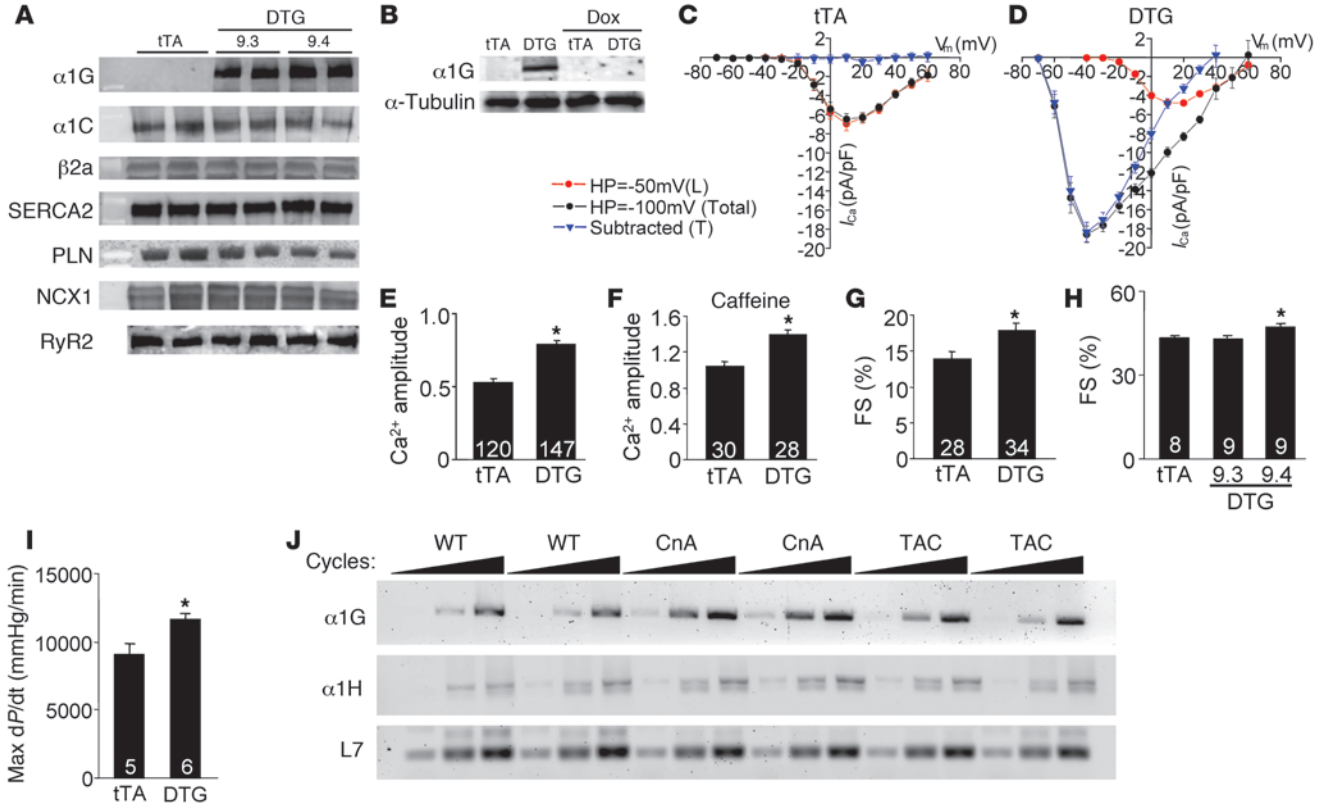

Figure 1

Generation of inducible transgenic mice with increased TTCC current. (**A**) Western blot analysis of α1G subunit protein in 2 independent DTG lines (9.3 and 9.4) without Dox (induced state). Levels of α1C, β2a, SERCA2, PLN, NCX1, and RyR2 were unchanged. (**B**) Western blot showing inducible expression of α1G protein in line 9.4 DTG mice without Dox and its extinguishment by 3 weeks of Dox administration. (**C** and **D**) Current-voltage relationships measured with a holding potential (HP) of –50 mV and –100 mV in tTA (27 cells from 5 hearts) and DTG (30 cells from 5 hearts) adult ventricular cardiomyocytes (line 9.4). The blue triangles represent the subtracted difference as T-current. (**E**) Amplitude of Ca^{2+} transients from tTA (control) and DTG (line 9.4) cardiomyocytes. (**F**) SR Ca^{2+} content assessed by amplitude of Ca^{2+} with caffeine stimulation. (**G**) Assessment of adult myocyte fractional shortening (FS) after isolation from tTA and DTG (line 9.4) hearts. (**H**) Fractional shortening of whole hearts from tTA and DTG (both lines) mice by echocardiography. (**I**) Invasive hemodynamic measurement in tTA and DTG line 9.3 mice. (**J**) RT-PCR for α1G, α1H, and L7 (control) from hearts of mice that were WT, transgenic for the activated calcineurin mutant protein (CnA), or subjected to pressure overload by TAC. Increasing numbers of PCR cycles are designated by the triangles in **J**. The number in each bar indicates the number of measured cardiomyocytes or mice. *$P < 0.05$ vs. tTA control.

heart to control the cardiac hypertrophic response (16). Indeed, mice lacking *α1H* showed reduced cardiac hypertrophy after pressure overload stimulation, presumably due to the fact that there was less Ca^{2+} influx in a calcineurin-containing membrane signaling microdomain (16). In cell types other than cardiomyocytes, TTCC-dependent Ca^{2+} can also signal cellular proliferation (18).

Here we show that overexpression of α1G in the heart has a very prominent effect on the hypertrophic response, consistent with the hypothesis that this channel regulates signaling within defined microdomains or through association with specific Ca^{2+}-activated signaling proteins. However, we paradoxically observed that increased TTCC current through α1G served an anti-hypertrophic and protective function in the heart, despite increasing Ca^{2+} influx. Consistent with this result, deletion of the *α1G* gene in mice rendered the heart more susceptible to cardiac hypertrophy and pathological remodeling. We show that part of the mechanism whereby α1G protects the heart is through regulation of NOS3, a Ca^{2+}-activated signaling effector that is known to alter the cardiac hypertrophic response (19).

Results

Generation of α1G-overexpressing transgenic mice. Here we generated inducible, cardiac-specific transgenic mice expressing α1G to determine the function of T-current reexpression during pathologic stimulation. Heart-specific and inducible expression was achieved with a binary α–myosin heavy chain (α-MHC) promoter–based transgene strategy (20). The responder transgene permitted expression of α1G in the heart only in the presence of the driver transgene encoding the tetracycline transactivator (tTA) protein in the absence of tetracycline/doxycycline (tetracycline/Dox) (Figure 1, A and B). Two responder lines were extensively analyzed, and both showed abundant protein overexpression in the heart with the tTA transgene (double transgenic [DTG]; Figure 1A). Administration of Dox completely eliminated expression of α1G protein in DTG mice (Figure 1B). Overexpression of α1G in the heart did not affect expression of the LTCC α1C or β2a subunits, nor were sarco/endoplasmic reticulum Ca^{2+}-ATPase (SERCA2), phospholamban (PLN), Na^{+}/Ca^{2+} exchanger 1 (NCX1), or ryanodine receptor 2 (RyR2) altered (Figure 1A).

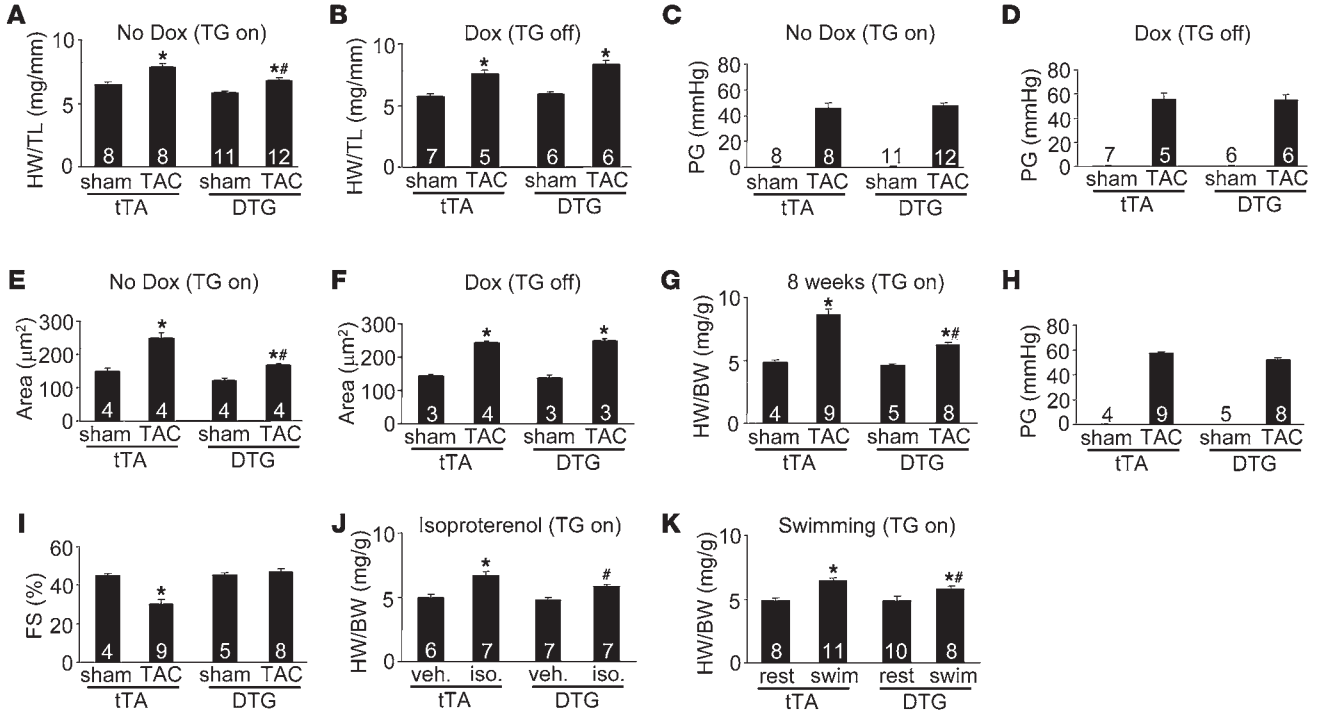

Figure 2

Targeted overexpression of α1G antagonizes cardiac hypertrophy after stress stimulation. (**A**) Heart weight (HW) normalized to tibia length (TL) for tTA and DTG (line 9.4) mice 2 weeks after sham surgery or TAC without Dox (transgene induced). (**B**) HW/TL for tTA and DTG (line 9.4) mice 2 weeks after sham surgery or TAC with Dox (transgene inhibited). (**C** and **D**) Systolic pressure gradient (PG) across the aortic constriction in mice without Dox (induced) (**C**) or with Dox (inhibited) (**D**). (**E** and **F**) Histological analysis of myocyte cross-sectional areas from ventricles (of the indicated groups of mice 2 weeks after TAC without Dox (induced) (**E**) or with Dox (inhibited) (**F**). (**G**) HW normalized to BW for tTA and DTG (line 9.4) mice 8 weeks after TAC without Dox (induced). (**H**) Systolic pressure gradient across the aortic constriction from the mice in **G**. (**I**) Fractional shortening assessment by echocardiography from the mice in **G**. (**J**) HW/BW in the indicated groups of mice after 2 weeks of isoproterenol infusion or PBS (veh.) without Dox (induced). (**K**) HW/BW after 3 weeks of swimming in the indicated groups of mice without Dox (induced). rest, resting. The number of mice analyzed in each group is shown within the bars. *$P < 0.05$ versus sham/veh./rest in the same mouse group; #$P < 0.05$ versus tTA subjected to TAC/isoproterenol/swimming.

However, LTCC current was reduced by approximately 15% in DTG myocytes (Figure 1, C and D).

We previously demonstrated that ventricular myocytes from α1G-overexpressing DTG mice exhibit robust T-currents (21). In separate patch-clamp experiments we show that myocytes from DTG mice have dramatic reexpression of TTCC current, compared with no current from tTA control mice (Figure 1, C and D). This dramatic induction in TTCC current affected contractile Ca^{2+} pools, since the amplitude of the Ca^{2+} transient was increased, as was sarcoplasmic reticulum (SR) Ca^{2+} load and fractional shortening of individual DTG myocytes in isolation (Figure 1, E–G). The augmentation in Ca^{2+} also enhanced ventricular performance and contractility in DTG mice as measured by echocardiography and a pressure-transducing catheter (Figure 1, H and I). Despite this enhancement in Ca^{2+} influx and contractility in hearts of DTG mice, pathology was not observed. Heart weight normalized to body weight was not increased at 3 or 8 months of age, nor was there induction of fibrosis in the heart or induction of the fetal gene program (Supplemental Figure 1, A–D; supplemental material available online with this article; doi:10.1172/JCI39724DS1). These results indicate that α1G overexpression in the heart enhances Ca^{2+} cycling and contractility without inducing pathology or a stress response.

Overexpression of α1G, as apposed to α1H, appears to model changes in gene expression that occur in the mouse heart during hypertrophy. More specifically, RT-PCR analysis of α1G and α1H mRNA levels in hearts of hypertrophic calcineurin-transgenic mice and WT mice subjected to pressure overload stimulation by transverse aortic constriction (TAC) showed substantial upregulation of α1G but only very mild upregulation of α1H compared with nonhypertrophic WT hearts (Figure 1J). These results suggest that α1G may play a greater role in affecting cardiac pathophysiology compared with α1H.

α1G-overexpressing DTG mice are protected from cardiac hypertrophy. Since increased Ca^{2+} influx is typically associated with cardiac hypertrophy (4), we initially hypothesized that pressure overload stimulation of α1G DTG mice would uncover an increased propensity toward hypertrophy or cardiomyopathy. However, α1G DTG mice without Dox (induced) showed significantly and surprisingly less cardiac hypertrophy after 2 weeks of TAC compared with tTA single-transgenic controls or DTG mice on Dox (uninduced) (Figure 2, A and B). All groups of mice subjected to TAC showed the same relative pressure gradients across the aortic constrictions (Figure 2, C and D). Assessment of myocyte cross-sectional surface areas also showed significantly less cellular hypertrophy in α1G DTG mice without Dox (induced) compared with single tTA

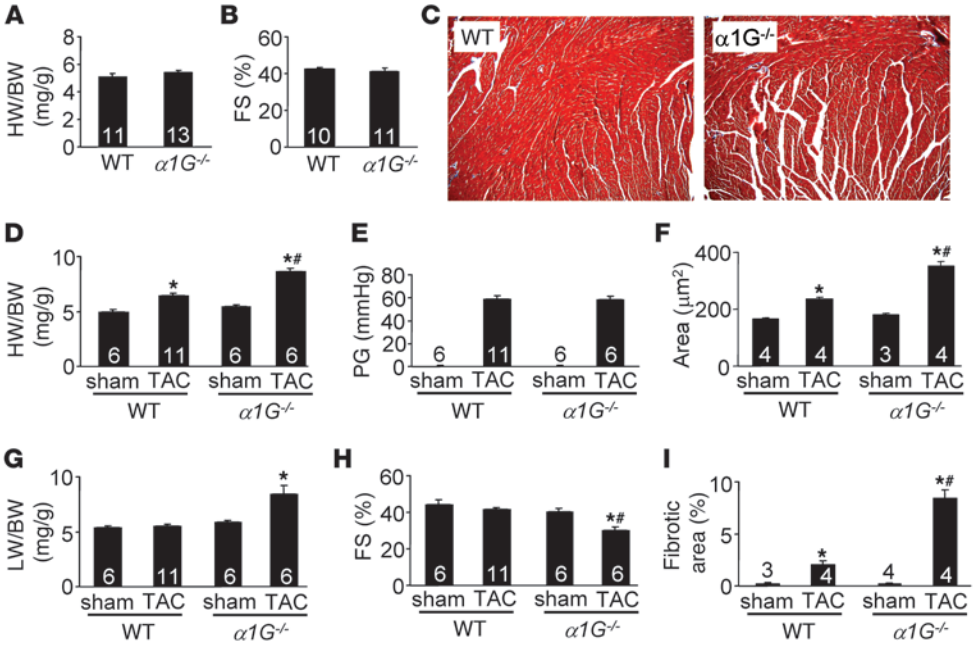

Figure 3

α1G deletion exacerbates cardiac hypertrophy 2 weeks after pressure overload. (**A**) HW/BW ratio of $\alpha 1G^{-/-}$ or $\alpha 1G^{+/+}$ (WT) mice at 10 weeks of age. (**B**) Fractional shortening assessment by echocardiography for $\alpha 1G^{-/-}$ or WT mice at 10 weeks of age. (**C**) Histological assessment (original magnification, ×100) of cellular pathology of $\alpha 1G^{-/-}$ or WT mice by Masson's trichrome staining at 10 weeks of age. (**D**) HW/BW ratio of $\alpha 1G^{-/-}$ or WT mice 2 weeks after sham surgery or TAC. (**E**) Systolic pressure gradient across the aortic constriction assessed by Doppler echocardiography in mice from **D**. (**F**) Histological analysis of myocyte cross-sectional areas from ventricles of mice in **D**. (**G**) Lung weight (LW) normalized to BW of mice in **D**. (**H**) Fractional shortening assessed by echocardiography for mice in **D**. (**I**) Quantitation of fibrotic area (blue) from Masson's trichrome–stained cardiac histological sections for mice in **D**. The number of mice analyzed in each group is shown within the bars. $^{*}P < 0.05$ versus sham; $^{\#}P < 0.05$ versus WT TAC.

transgenic controls or DTG mice with Dox (uninduced) (Figure 2, E and F). The same significant reduction in cardiac hypertrophy was observed in α1G DTG mice subjected to TAC stimulation for 8 weeks, which also had equal pressure gradients measured at 1 week after TAC (Figure 2, G and H). Interestingly, after 8 weeks of TAC, single tTA transgenic mice began to show signs of failure, such as a significant reduction in fractional shortening, which was not observed in α1G DTG mice (Figure 2I). Finally, we also extended these observations by employing 2 other models of hypertrophy: 2 weeks of isoproterenol infusion with Alzet minipumps or 3 weeks of forced swimming. Remarkably, α1G DTG mice (no Dox) showed less cardiac hypertrophy to isoproterenol infusion and swimming exercise compared with tTA single-transgenic mice (Figure 2, J and K). Collectively, these results indicate that increased TTCC current associated with α1G overexpression antagonizes pathologic and physiologic cardiac hypertrophic responses.

That α1G overexpression is cardioprotective was completely unexpected given our previous observations with inducible β2a-overexpressing transgenic mice, which exhibit hypertrophic cardiomyopathy due to increased LTCC current and associated Ca^{2+} influx (8). Here we extended these data by conducting a set of experiments in which the β2a inducible transgene was activated for the first time in young adulthood by removal of Dox at weaning (Supplemental Figure 2A). Compared with β2a DTG mice that always expressed the transgene (fetal and neonatal expression), adult induction of β2a showed no signs of cardiac hypertrophy, reductions in functional performance, or fibrosis (Supplemental Figure 2, B–F). However, adult induction of β2a expression in the heart promoted greater hypertrophy, greater increases in cellular surface areas, loss of ventricular performance, and pulmonary edema after TAC stimulation (Supplemental Figure 3, A–E). Thus, increased Ca^{2+} influx through the LTCC enhances hypertrophy and is pathologic to the heart, in dramatic contrast to the effect observed with increased TTCC current, suggesting that these two pools of Ca^{2+} are functionally distinct. We also crossed α1G and β2a transgenic lines together, predicting that enhanced TTCC current might protect against the negative effects of augmented LTCC current. However, we observed no reduction in heart disease, suggesting that β2a-enhanced LTCC Ca^{2+} influx is pathologic to the heart through a unique signaling domain that is not affected by TTCC (data not shown).

$\alpha 1G^{-/-}$ mice are more susceptible to cardiac hypertrophy and pathology. $\alpha 1G^{-/-}$ mice were previously reported to display mild bradycardia and slowing of atrioventricular conduction, but no other cardiac pathology (22). Extensive baseline analysis of $\alpha 1G^{-/-}$ mice in our hands revealed no alterations in heart size, geometry, ventricular function, or defects in cellular architecture or fibrotic content at 10 weeks of age (Figure 3, A–C). Consistent with the reduction in hypertrophy observed after TAC in α1G DTG mice, $\alpha 1G^{-/-}$ mice showed the antithetical response of greater cardiac hypertrophy after 2 weeks of TAC stimulation, with equal pressure gradients across the constrictions (Figure 3, D and E). Histological analysis of hearts showed greater increases in cell-surface areas after TAC in hearts of $\alpha 1G^{-/-}$ mice compared with controls (Figure 3F). $\alpha 1G^{-/-}$ mice also developed pulmonary edema, decreased ventricular performance, and a substantial fibrotic response after TAC compared with WT controls (Figure 3, G–I). Pressure overload in the mouse heart is known to induce TTCC current in ventricular myocytes (16), and our data suggest that this effect through α1G antagonizes the hypertrophic response and is normally cardioprotective.

In addition being subjected to pressure overload stimulation, $\alpha 1G^{-/-}$ mice were stimulated to undergo hypertrophy by isoproterenol infusion and swimming exercise. Consistent with the TAC experiments, isoproterenol infusion over 2 weeks induced greater pathologic hypertrophy in $\alpha 1G^{-/-}$ mice, greater ventricular fibrosis, and a significant reduction in ventricular performance compared with WT, strain-matched controls (Figure 4, A–D). However, exer-

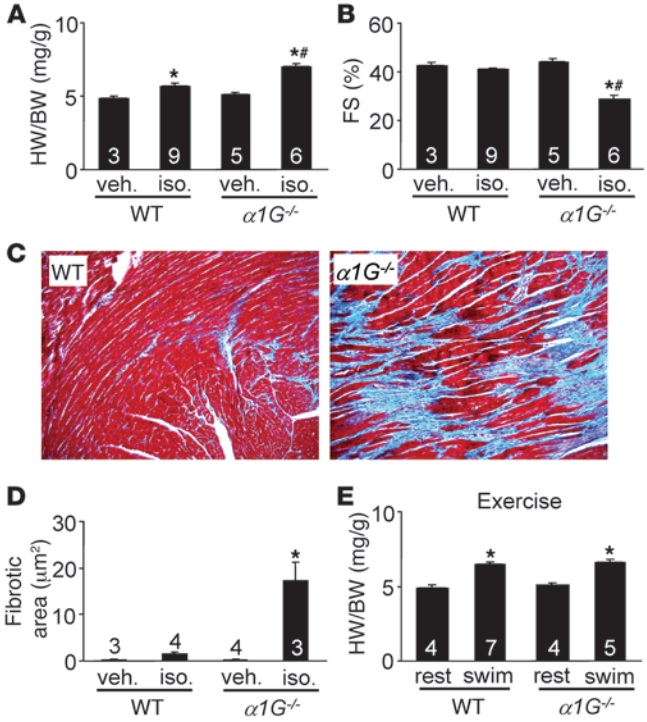

Figure 4
α1G deletion exacerbates cardiac pathology after isoproterenol infusion. (**A**) HW/BW in $\alpha 1G^{-/-}$ or $\alpha 1G^{+/+}$ (WT) mice infused with isoproterenol (iso.) at 60 mg/kg/d or PBS for 14 days. (**B**) Fractional shortening (FS) assessment by echocardiography from mice as in **A**. (**C**) Representative histological assessment (original magnification, ×100) of pathology from mice as in **A**. (**D**) Quantitation of fibrotic area (blue) from Masson's trichrome–stained cardiac histological sections obtained from mice as in **A**. (**E**) HW/BW after 3 weeks of swimming exercise in the indicated groups of mice. The number of mice analyzed in each group is shown within the bars. $^{*}P < 0.05$ versus WT veh./rest; $^{\#}P < 0.05$ versus WT iso.

cise-induced hypertrophy was not exacerbated by the loss of *α1G*, suggesting specificity for the pathologic hypertrophic response (Figure 4E). Indeed, physiologic hypertrophy (exercise) does not reactivate the fetal gene program and would not be predicted to induce TTCC current, so its loss from the heart during exercise is inconsequential. However, overexpression of α1G might still antagonize physiologic hypertrophy by inhibiting an upstream nodal signaling pathway (see below). In summary, the data suggest that TTCC current is protective to the myocardium during pathologic insults, when the current is normally reexpressed.

α1G regulates the hypertrophic response in a myocyte-autonomous manner. That $\alpha 1G^{-/-}$ mice developed greater cardiac hypertrophy following TAC or isoproterenol infusion could be due to loss of this protein in the vasculature or other non-myocytes. To address this concern, we crossed the α1G transgene (with tTA) into the $\alpha 1G^{-/-}$ background and performed TAC stimulation. The greater increase in cardiac hypertrophy due to total somatic deletion of *α1G* was rescued by the myocyte-specific α1G transgene (Figure 5, A and B). Indeed, the $\alpha 1G^{-/-}$ mice with the α1G transgene responded very similarly to α1G DTG mice, indicting that the pro-hypertrophic affect associated with *α1G* deletion was due to a myocyte-autonomous signaling mechanism. Importantly, deletion of *α1G* did not alter the expression of α1G protein driven by the transgene (Figure 5C). Also, the decrease in cardiac function observed in $\alpha 1G^{-/-}$ mice after TAC was rescued by α1G overexpression (Figure 5D).

α1G interacts with NOS3 as an anti-hypertrophic signaling mechanism. We have shown that α1G predominantly localizes outside the T-tubular network, while LTCCs reside both in the T-tubules and outer sarcolemma to regulate ECC (21). Thus, we hypothesized that α1G reexpression in the heart provides local Ca^{2+} at the level of the sarcolemma in defined signaling domains to activate one or more anti-hypertrophic effectors. The most obvious anti-hypertrophic signaling pathway that is Ca^{2+} activated involves NOS3 at the sarcolemma (caveolae) where it generates local NO to induce soluble guanylyl cyclase and cGMP production, which has an anti-

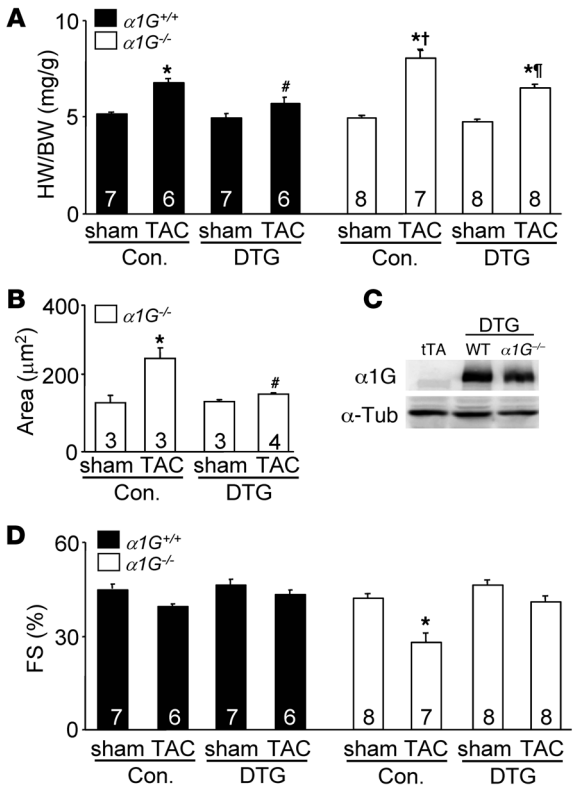

Figure 5
Restoration of α1G in cardiomyocytes suppresses the pathologic phenotype of $\alpha 1G^{-/-}$ mice. (**A**) HW/BW of α1G DTG (line 9.4) or control (WT and tTA) mice in the $\alpha 1G^{-/-}$ or $\alpha 1G^{+/+}$ background 2 weeks after a sham or TAC procedure. (**B**) Histological analysis of myocyte cross-sectional areas from ventricles of α1G DTG (line 9.4) or control (Con.; WT and tTA) mice in the $\alpha 1G^{-/-}$ background 2 weeks after TAC. (**C**) Western blot analysis of α1G protein expression from α1G DTG (line 9.4) mice in the $\alpha 1G^{-/-}$ or $\alpha 1G^{+/+}$ backgrounds at 3 months of age. α-Tub, α-tubulin. (**D**) Fractional shortening assessment by echocardiography from mice as in **A**. The number of mice analyzed in each group is shown within the bars. $^{*}P < 0.05$ versus sham; $^{\#}P < 0.05$ versus control TAC in the $\alpha 1G^{+/+}$ background; $^{\dagger}P < 0.05$ versus control TAC in the $\alpha 1G^{+/+}$ background; $^{\P}P < 0.05$ versus control TAC in the $\alpha 1G^{-/-}$ background.

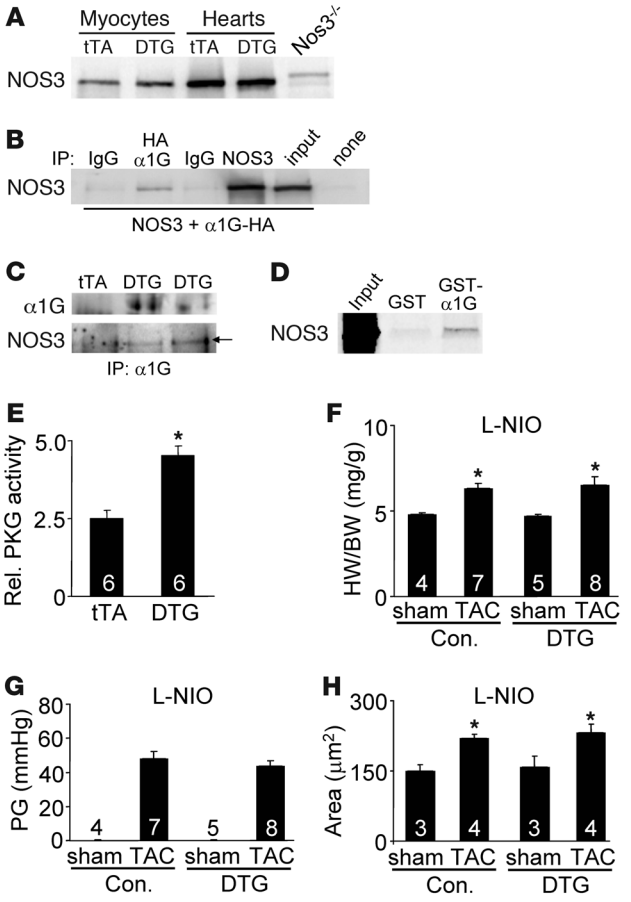

Figure 6

NOS3 is involved downstream of α1G. (**A**) Western blot analysis for NOS3 expression from isolated adult cardiomyocytes or whole hearts of tTA or DTG (line 9.4) mice. A *Nos3*$^{-/-}$ heart sample is shown as a negative control. (**B**) Western blot for NOS3 after immunoprecipitation for HA-tagged α1G and associated NOS3 after transient transfection into HEK293 cells. "None" indicates input from HEK cells transfected with an HA-encoding empty vector. (**C**) Immunoprecipitation from tTA or DTG hearts that were subjected to pressure overload. α1G antibody was used for the immunoprecipitation, followed by Western blotting for α1G and NOS3 protein. (**D**) Autoradiogram of [^{35}S]NOS3 protein association with α1G using bacteria-generated GST or GST-α1G fusion protein. (**E**) PKGI activity assay from tTA and DTG hearts after pressure overload. Rel., relative. **P* < 0.05 versus tTA. (**F**) HW/BW ratio of α1G DTG (line 9.4) and control (tTA and WT) mice 2 weeks after sham surgery or TAC with administration of L-NIO. (**G**) Systolic pressure gradient across the aortic constriction from mice as in **F**. (**H**) Histological analysis of myocyte cross-sectional areas from ventricles of mice in **F**. The number of mice analyzed in each group is shown within the bars. **P* < 0.05 versus sham control.

hypertrophic effect through cGMP-dependent protein kinase type I (PKGI) (23, 24). NOS3 protein was identified in the heart and purified adult myocytes from tTA and α1G DTG mice, although we detected no differences in total protein levels or serine 1,177 phosphorylation (Figure 6A and data not shown). However, NOS3 can be activated independent of phosphorylation through a direct effect of Ca^{2+}. Indeed, we observed that immunoprecipitation of α1G (HA-tagged) from overexpressing cells pulled down NOS3, consistent with a known localization of each protein to caveola-containing membrane domains (10, 25) (Figure 6B). Of note, α1H specifically immunoprecipitated with NOS3 as well from cells overexpressing each protein (data not shown). NOS3 was also specifically immunoprecipitated from α1G DTG hearts after TAC stimulation, but not from tTA control hearts (Figure 6C). This interaction between α1G and NOS3 is likely direct, since bacteria-generated glutathione *S*-transferase–α1G (GST-α1G) fusion protein, but not GST alone, pulled down NOS3 generated in a cell-free transcription-translation reaction (Figure 6D). In fact, using deletion fragments of α1G, we identified specific interactions in both the N (amino acids 1–79) and C termini (amino acids 1,861–2,290) of α1G for NOS3 binding (data not shown). Downstream of NOS3, which is presumably activated by TTCC current, we observed significantly greater activation of PKGI in α1G DTG hearts after TAC stimulation (Figure 6E). We also observed a trend toward greater cGMP levels and citrulline formation in α1G hearts from mice subjected to TAC stimulation, suggesting that the entire putative anti-hypertrophic pathway was augmented (data not shown).

To further evaluate the potential involvement of NOS3 as a recipient of α1G-dependent Ca^{2+} within a select signaling microdomain (hence difficult to detect), we employed L-N^5-(1-iminoethyl)ornithine hydrochloride (L-NIO), a selective NOS3 inhibitor, as well as *Nos3*$^{-/-}$ mice. We treated tTA control and α1G DTG mice with L-NIO at 40 mg/kg/d for 2 weeks during TAC stimulation. Remarkably, L-NIO treatment reversed the anti-hypertrophic effect associated with α1G overexpression, so that hearts from DTG mice hypertrophied to the same extent as tTA controls (Figure 6, F and H). Importantly, there were no differences in the pressure gradient across the aortic constriction (Figure 6G), nor did L-NIO alter the TTCC current associated with the α1G transgene in adult myocytes (data not shown). These results indicate that L-NIO treatment specifically reversed the effect of increased TTCC expression on the hypertrophic response, suggesting that NOS3 may be a critical downstream anti-hypertrophic effector of this Ca^{2+} signal.

Given concerns over drug specificity, α1G DTG mice were also crossed into the *Nos3*$^{-/-}$ background, which did not alter expression of α1G protein regulated by the double transgenes (Figure 7A). However, consistent with the effects of L-NIO treatment, loss of *Nos3* reversed the anti-hypertrophic effect of α1G overexpression, such that DTG mice now developed as much hypertrophy at the cellular and whole-organ level as controls (Figure 7, B and D). Once again, pressure gradients across the aortic constriction were not different (Figure 7C). Mechanistically, increased TTCC current resulted in a 15% downregulation in LTCC current in adult myocytes (Figure 1, C and D), and since increased LTCC current can enhance cardiac hypertrophy following pressure overload stimulation, the results suggested another means whereby α1G overexpression might be anti-hypertrophic. However, loss of *Nos3* (null mice) did not restore the loss of LTCC current in α1G DTG myocytes, even though the greater hypertrophy profile after TAC was restored (Figure 7E). Similarly L-NIO treatment did not increase LTCC current to WT values in α1G DTG myocytes at baseline, despite reversing the inhibition of hypertrophy, again suggesting that the anti-hypertrophic mechanism of α1G is not largely due to downregulation of LTCC (Figure 7F). The simplest explanation for these results is that α1G provides local Ca^{2+} to a regional pool of NOS3 that signals through known pathway constituents in reduc-

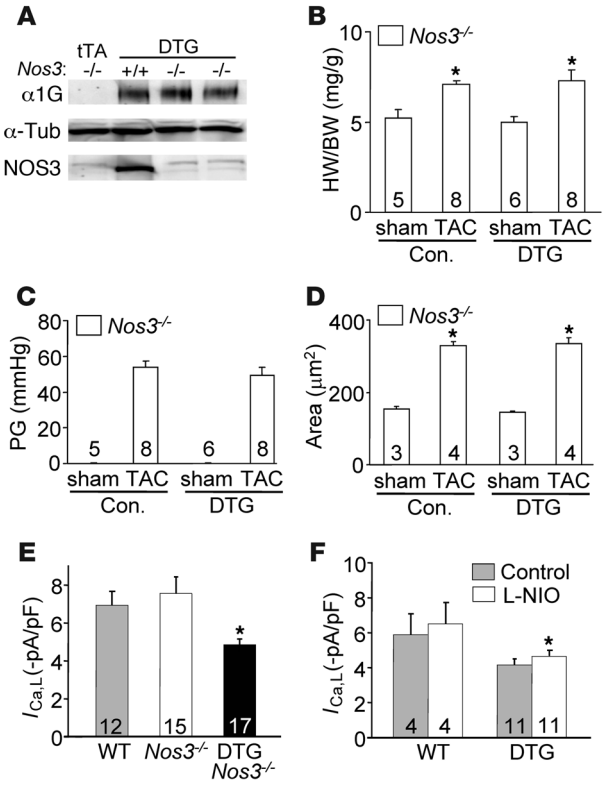

Figure 7
NOS3 ablation abolishes the anti-hypertrophic effect caused by α1G overexpression. (**A**) Western blot analysis of α1G, α-tubulin (control), and NOS3 from α1G DTG (line 9.4) mice in the *Nos3*$^{-/-}$ or *Nos3*$^{+/+}$ backgrounds at 3 months of age. (**B**) HW/BW in α1G DTG (line 9.4) and control (tTA and WT) mice in the *Nos3*$^{-/-}$ background 2 weeks after a sham or TAC procedure. (**C**) Systolic pressure gradient across the aortic constriction in mice from **B**. (**D**) Histological analysis of myocyte cross-sectional areas from ventricles of mice in **B**. The number of mice analyzed in each group is shown within the bars. *P < 0.05 versus sham control. (**E**) Peak L-type Ca^{2+} current of adult myocytes isolated from hearts of the indicated groups of mice. Values were collected at a holding potential of –40 mV and test potentials of +20 mV. Numbers in the bars represent the numbers of myocytes analyzed. *P < 0.05 versus WT. (**F**) Peak L-type Ca^{2+} current of adult myocytes isolated from hearts of the indicated groups of mice treated with or with out L-NIO. Numbers in the bars represent the numbers of myocytes analyzed. *P < 0.05 versus WT.

ing the hypertrophic response. However, one area of caution is that L-NIO and deletion of *Nos3*$^{-/-}$ could have secondarily impacted the hypertrophic response, such as through an increase in blood pressure or local vasoconstriction, events that could have complicated the interpretation of our rescue results.

Discussion

Cardiomyocyte contraction is regulated by a highly specialized system of Ca^{2+} channels, pumps, and exchangers (26). The contractile cycle begins by depolarization of the sarcolemma and activation of the voltage-dependent LTCCs that reside in a specialized contractile domain adjacent to ryanodine receptors embedded within the SR. LTCCs may also reside outside the RyR2-containing junctional complex region, such as within caveolae whereby Ca^{2+} influx could control reactive signaling effectors (6). We have previously shown that LTCC β2a subunit overexpression in transgenic mice, which produced large increases in Ca^{2+} influx, could signal pathologic hypertrophic remodeling, similar to what was observed with α1C subunit overexpression of the LTCC, or the combination of α1C with β2a (7, 8, 27). These results suggest that increased Ca^{2+} influx by LTCCs was pathologic, consistent with our results here showing exacerbated hypertrophy following TAC stimulation or isoproterenol infusion in β2a DTG mice (Supplemental Figure 3). Similarly, increased Ca^{2+} influx in myocytes through transient receptor potential canonical (TRPC) channels, which mediate store-, receptor-, and stretch-operated Ca^{2+} entry (28–31), can induce pathologic hypertrophy through a calcineurin-dependent pathway (32–34). Similarly, we have shown that overexpression of PMCA4b, which presumably removes Ca^{2+} from defined sarcolemmal microdomains involved in signaling to calcineurin, could reduce the cardiac hypertrophic response (9). Thus, a case can be made that any increase in Ca^{2+} influx, whether contractile or microdomain associated, can induce or exacerbate the cardiac hypertrophic response through known Ca^{2+}-sensitive signaling effectors such as calcineurin.

Most unexpectedly, we observed that increased Ca^{2+} influx associated with α1G overexpression did not induce a hypertrophic response or pathology or even sensitize to greater hypertrophy with stimulation. In contrast, α1G overexpression was protective and antagonized the hypertrophic response and the transition to heart failure. We have previously shown that these α1G-overexpressing transgenic mice have greater Ca^{2+} influx during the contractile cycle using 3 different techniques (21). Here we report that α1G transgenic mice also showed greater Ca^{2+} transients and SR Ca^{2+} load and enhanced cardiac contractile performance. These latter observations were somewhat unexpected, as it is generally accepted that physiologic reexpression of TTCCs in the heart does not affect ECC (10, 21). However, we believe that the mild increase in contractility in α1G-overexpressing mice is most likely due to the relatively high levels of overexpression that were achieved, leading to Ca^{2+} "spillover" outside the presumed signaling microdomain, loading the SR with more Ca^{2+}. TTCCs are expressed in ventricular myocytes during fetal and early neonatal development, when they likely contribute to contractility, especially since the T-tubular network has yet to be fully established (10, 35). Thus, TTCCs can affect contractility in immature myocytes, although in the adult ventricular myocyte the small increase in current that is typically observed upon disease-induced reexpression is unlikely to regulate contractile function and may be more dedicated to signaling. Indeed, in vascular smooth muscle cells, TTCC current plays a prominent role in selectively regulating proliferation, as in many other non-muscle cell types (18, 36, 37).

We observed that increased Ca^{2+} influx associated with α1G overexpression antagonized the hypertrophic response, while *α1G*$^{-/-}$ mice showed more hypertrophy and disease after stimulation. These results are seemingly in contrast to recently published data in *α1H*$^{-/-}$ mice (16). *α1H*$^{-/-}$ mice subjected to TAC stimulation showed less cardiac hypertrophy than controls, while *α1G*$^{-/-}$ mice showed a hypertrophic response that was statistically similar to that of WT controls (16). On the surface, the results of Chiang et al. suggest that TTCC reexpression is pathologic and that it contributes to hypertrophy by adding more Ca^{2+} from α1H channels. While we cannot explain why Chiang et al. did not observe more hypertrophy in *α1G*$^{-/-}$ mice, as we observed, the reduction in hypertrophy seen in *α1H*$^{-/-}$ mice could be explained by functional differences between α1G and α1H. For example, although all 3 TTCCs (α1G, α1H, α1I) generate current characteristics that are relatively similar, each has unique structural and kinetic features that suggest some specialization in function (10). CaMKII increases T-type current from α1H but not α1G (38). α1H may be partially regulated by Ca^{2+} (although not as much as Ca^{2+} regulates LTCCs), while α1G and α1I are insensitive to Ca^{2+} feedback (39). α1H, but not α1G, is inhibited by the $G_{\beta\gamma}$ subunit following G protein activation, suggesting a unique link to membrane receptor signals in the regulation of T-type current (40). Lysophosphatidylcholine also specifically augments α1H, but not α1G, Ca^{2+} current (41). Given these observations, it is possible that α1G participates in a Ca^{2+} signaling microdomain that is anti-hypertrophic, while α1H is pro-hypertrophic through a different signaling microdomain. It is also plausible that α1G and α1H activate unique signaling factors in the same microdomain through direct protein-protein interactions that are specific to each channel. However, it is unlikely that NOS3 signaling explains these results, since α1H also interacted with NOS3 in our immunoprecipitation experiments, suggesting that it is part of the same signaling microdomain with α1G (data not shown).

Our data suggest a working model for a novel signaling circuit in which reexpressed α1G during pathologic cardiac hypertrophy binds to NOS3 to provide a local Ca^{2+} signal that induces NOS3 activation and a subsequent anti-hypertrophic effect through local cGMP and PKGI signaling in defined microdomains. By comparison, the atrial natriuretic factor/B-type natriuretic peptide (ANF/BNP) receptor generates cGMP that can also antagonize cardiac hypertrophy and provide protection to the heart (42). Increasing total cardiac cGMP levels with sildenafil also antagonizes the cardiac hypertrophic response to pressure overload stimulation (43). Interestingly, TTCCs were shown to regulate NO-cGMP–induced smooth muscle relaxation and contraction responsible for penile erection control (44). In its coupled state of activation, NOS3 signaling has been shown to be protective and anti-hypertrophic (45–47). Indeed, *Nos3*$^{-/-}$ mice become hypertrophic with aging and show greater hypertrophy following pressure overload stimulation (45–48). NOS3-overexpressing transgenic mice also showed less secondary hypertrophic remodeling after myocardial infarction (48). However, extreme activation of NOS3 can have detrimental effects by generating an uncoupled state, such that maladaptive and pro-hypertrophic reactive oxygen species are produced (49).

NOS3 is likely to be only part of the mechanism whereby α1G TTCC current reexpression exerts its protective and anti-hypertrophic effect. For example, we consistently identified activation of CaMKII in the hearts of α1G transgenic mice (data not shown), although this effect is of unknown relevance to the hypertrophic response here. Future studies will be important to determine other potential mechanisms whereby TTCC current may be cardioprotective, as well as to further investigate how α1G and α1H might function differently in the heart. At the very least, our data indicate that α1G-dependent signaling is protective to the heart, and a better understanding of the downstream mechanisms could suggest novel therapeutic approaches for treating human heart disease. Finally, the data presented here show only a partial effect on the cardiac hypertrophic response by either deletion or overexpression of α1G, clearly indicating that this TTCC/NOS3/PKGI pathway is only a component of a much more complicated and multifactorial biologic response that regulates cardiac hypertrophy. Thus, identification of additional protective and anti-hypertrophic pathways will also be important in our efforts to understand and treat human heart disease.

Methods

Transgenic mice. A cDNA for mouse α1G (Cav3.1; gift from Norbert Klugbauer, Albert-Ludwigs Universität, Freiburg, Germany) was cloned into the murine inducible α-MHC promoter expression vector (20). The tTA single-transgenic line used in conjunction with the α1G responder transgene to generate Dox-regulated expression was described previously (20). *α1G* gene–targeted mice were described previously (50). *Nos3* gene–targeted mice were obtained from The Jackson Laboratory. Experiments involving animals were approved by the Institutional Animal Care and Use Committee of Cincinnati Children's Hospital.

Western blot analysis and PKGI activity. Western blot analysis of mouse ventricle homogenates was performed as previously reported (32). Briefly, membrane-rich fractions were prepared in extraction buffer (250 mM sucrose, 10 mM Tris-HCl pH 7.5, 1 mM DTT with protease inhibitors; Roche). Heart samples were homogenized in extraction buffer with a motor-driven Teflon homogenizer; homogenates were centrifuged at 3,000 *g* for 5 minutes at 4°C; and resultant supernatants were centrifuged at 28,000 *g* for 30 minutes to generate the final protein extracts. Antibodies included α1G subunit (custom made from YenZym), β2a subunit (gift from Kevin P. Campbell, University of Iowa, Iowa City, Iowa), α1C subunit (Alomone Labs Ltd.), NCX1 (Swant Inc.), SERCA2, α-tubulin, ryanodine receptor 2 (Santa Cruz Biotechnology Inc.), PLN (Affinity BioReagents), GAPDH (Research Diagnostics Inc.), and NOS3 (BD). Chemifluorescence detection was performed with the Vistra ECF reagent (Amersham Pharmacia Biotech) and scanned with a Storm 860 PhosphoImager (GE Medical). PKGI activity was assayed with a colorimetric-based kit according to the manufacturer's recommendation from whole heart protein homogenates (CycLex Co.).

Isolation of adult cardiomyocytes and Ca^{2+} measurements. Ca^{2+}-tolerant cardiomyocytes were selected following a standard isolation procedure from whole hearts placed in Tyrode solution with additives (120 mM NaCl, 5.4 mM KCl, 1.2 mM NaH_2PO_4, 5.6 mM glucose, 20 mM $NaHCO_3$, 1.6 mM $MgCl_2$, 10 mM 2,3-butanedione monoxime [BDM], and 5 mM taurine; buffer A) and gassed with 95% O_2 and 5% CO_2. Hearts were then perfused with buffer A containing 1 mg/ml collagenase type II (Worthington) and 0.08 mg/ml protease type XIV (Sigma-Aldrich) at 37°C (10–14 minutes total). After perfusion, the ventricles were disassociated into individual myocytes, filtered, and incubated with 2 μM Fura-2 acetoxymethyl ester (Invitrogen) for 30–35 minutes in buffer C (buffer A with 1 mM Ca^{2+} without BDM) at room temperature. After being loaded, the cells were washed and resuspended in buffer C. After 3 washes (40 minutes), the cells were placed in a Plexiglas chamber containing 500 μl of fresh buffer C. The Fura-2 fluorescence ratio was determined at room temperature using a Delta Scan dual-beam spectrofluorophotometer (Photon Technology International), operated at an emission wavelength of 510 nM with excitation wavelengths

of 340 and 380 nM. The stimulating frequency for Ca^{2+} transient measurements was 0.5 Hz. Baseline amplitude (estimated by 340 nM/380 nM ratio) of the Ca^{2+} signal was acquired, and data were analyzed using from Felix 1.1 and IonWizard (IonOptix) software.

Measurement of L-type and T-type calcium current using patch clamp methods. For patch clamp experiments, after perfusion, the ventricles were separated from the atria, minced, and gently agitated in low Cl^-, high K^+ Kraft-Bruhe (KB) solution consisting of 50 mM glutamic acid, 40 mM KCl, 20 mM taurine, 20 mM KH_2PO_4, 3 mM $MgCl_2$, 10 mM glucose, 1 mM EGTA, 10 mM HEPES pH 7.4. The dissociated cells were filtered through a nylon mesh and stored at 4°C in KB solution until use. Only Ca^{2+}-tolerant cells with clear cross-striations and without spontaneous contractions or significant granulation were selected for the experiments. All patch clamp experiments were conducted at room temperature (20–23°C) using a patch clamp amplifier (Axopatch200A; Axon Instruments). The recorded currents (I_{Ca}) were filtered at 2 kHz through a 4-pole low-pass Bessel filter and digitized at 5 kHz. The experiments were controlled using pClamp 5.6 software (Axon Instruments) and analyzed using Clampfit 6.0.3. Current recordings were performed in bath solution superfused with the following Na^+-free solution: 2 mM $CaCl_2$, 5 mM 4-aminopyridine, 136 mM tetraethylammonium-Cl (TEA-Cl), 1.1 mM $MgCl_2$, 25 mM HEPES, and 22 mM glucose (pH 7.4 with TEA-OH). The pipette solution contained: 100 mM cesium aspartate, 20 mM CsCl, 1 mM $MgCl_2$, 2 mM Mg-ATP, 0.5 mM Na_2-GTP, 5 mM EGTA, 5 mM HEPES (pH 7.3 with 1N CsOH). The low-voltage activated T-type Ca^{2+} currents ($I_{Ca,T}$) were separated from high-voltage activated L-type Ca^{2+} currents ($I_{Ca,L}$) by subtracting the current differences between the traces from holding potentials of –100 mV (both $I_{Ca,T}$ and $I_{Ca,L}$ available) and –50 mV (only $I_{Ca,L}$ current available). $I_{Ca,T}$ and $I_{Ca,L}$ were measured by applying depolarizing voltage steps (380 ms) from –70 mV to +60 mV and –40 mV to +60 mV, respectively, in 10-mV increments. The NOS3 inhibitor L-NIO (10 μM) was used with 5 minutes perfusion before $I_{Ca,L}$ was elicited at a test potential of +20 mV from a holding potential of –40 mV.

RT-PCR, histological, and MetaMorph analysis. RT-PCR was performed as previously described (8). *α1G* and *α1H* mRNA was detected with the following specific primers: 5′-CAGCTGCCTGTCAACTCCCA-3′ and 5′-GAGTTCAGAAGAGGACCGGG-3′ for *α1G* and 5′-GTACTCACTGGCTGTGACCC-3′ and 5′-CTGCCCACCAAGTTGCGTGA-3′ for *α1H*. For histological analysis, hearts were collected at the indicated times, fixed in 10% formalin containing PBS, and embedded in paraffin. Serial 7-μm heart sections from each group were stained with H&E and Masson's trichrome (to detect fibrosis). Myocyte cross-sectional areas were analyzed in slides stained with wheat germ agglutinin–FITC conjugate at 50 μg/ml to accurately identify sarcolemmal membrane as previously reported (51). MetaMorph (Molecular Devices) analysis was performed as previously described for assessment of fibrosis (8). All assessments were performed in a blinded manner.

Echocardiography, invasive hemodynamics measurement, drug treatment, swimming test, and pressure overload. Mice from all genotypes or treatment groups were anesthetized with isoflurane, and echocardiography was performed using a Hewlett Packard 5500 instrument with a 15-MHz microprobe as previously described (32). Echocardiographic measurements were taken on M-mode in triplicate for each mouse. For invasive hemodynamics in the closed-chest mouse, a 1.4F Millar catheter was placed into the left ventricle through the right carotid artery to monitor real-time heart rate and arterial and left-ventricular pressures as well as $+dP/dt$ (dP/dt_{max}) and $-dP/dt$ (dP/dt_{min}) using PowerLab systems and Chart software (AD Instruments) as previously described (52). For pressure overload, 8- to 11-week-old male mice of each genotype were subjected to a TAC or sham surgical procedure as previously described (32). Pressure gradients across the constriction were measured by Doppler echocardiography as previously described (53). Alzet osmotic minipumps (no. 2002; Durect Corp) containing isoproterenol (60 mg/kg/d) or PBS were surgically inserted dorsally and subcutaneously in 2-month-old mice under isoflurane anesthesia as previously described (32). To shut down expression of α1G, DTG mice were given Dox (Sigma-Aldrich) at 1 g/l in drinking water for 3 weeks. For treatment with the NOS3-specific inhibitor L-NIO (Sigma-Aldrich), mice were given intraperitoneal administration at 40 mg/kg/d from 3 days before TAC until harvest. Swimming exercise for 21 days was described previously (54).

Immunoprecipitation and GST pull-down assay. cDNAs for HA-tagged mouse α1G and mouse NOS3 (obtained from Open Biosystems) were cloned into expression vectors and transfected into HEK293 cells using FuGENE 6 reagent (Roche Applied Sciences). Cells were lysed at 4°C in IP buffer (20 mM Tris-HCl pH 7.5, 250 mM NaCl, 1 mM DTT, 1% Triton X-100) containing protease and phosphatase inhibitors (Roche), followed by sonication. Lysates were cleared by centrifugation at 20,000 *g* for 10 minutes and then incubated with the indicated antibodies and protein A/G agarose beads (Santa Cruz Biotechnology Inc.) overnight at 4°C. The beads were washed extensively with binding buffer, and the proteins were resolved on a 7.5% SDS-PAGE for subsequent Western blotting.

To generate a GST fusion protein, we subcloned the mouse α1G cDNA into pGEX-4T-1 (Amersham Pharmacia Biotech). The GST fusion protein was expressed in *Escherichia coli* BL21 cells. Binding assays were performed with ^{35}S-labeled NOS3 protein synthesized in vitro by using the TnT Coupled Reticulocyte Lysate System (Promega) in the presence of [^{35}S]methionine (Amersham Biosciences). Equal amounts of immobilized GST fusion proteins were incubated for 2 hours at 4°C with 10 μl ^{35}S-labeled NOS3 in buffer. After 4 washes in buffer, beads were boiled in SDS sample buffer and resolved by SDS-PAGE, followed by autoradiography.

Statistics. All results are presented as mean ± SEM. Statistical analysis was performed using SigmaPlot 11.0 software for unpaired 2-tailed *t* test (for 2 groups) and 2-way ANOVA (for groups of 4–8). *P* values less than 0.05 were considered significant.

Acknowledgments

This work was supported by grants from the NIH (to J.D. Molkentin, J. Robbins, S.R. Houser, and A. Schwartz), as well as by an international grant in heart failure research from the Fondation Leducq and the Howard Hughes Medical Institute (to J.D. Molkentin). We thank Hee-Sup Shin (Korea Institute of Science and Technology, Seoul, South Korea) for allowing access to $\alpha 1G^{-/-}$ mice and Chien-Chang Chen (Academia Sinica, Taipei, Republic of China) for sending these mice from his colony.

Received for publication May 1, 2009, and accepted in revised form September 23, 2009.

Address correspondence to: Jeffery D. Molkentin, Cincinnati Children's Hospital Medical Center, Howard Hughes Medical Institute, Molecular Cardiovascular Biology, 240 Albert Sabin Way, MLC 7020, Cincinnati, Ohio 45229, USA. Phone: (513) 636-3557; Fax (513) 636-5958; E-mail: jeff.molkentin@cchmc.org.

1. Lorell, B.H., and Carabello, B.A. 2000. Left ventricular hypertrophy: pathogenesis, detection, and prognosis. *Circulation.* **102**:470–479.
2. Ho, K.K., Levy, D., Kannel, W.B., and Pinsky, J.L. 1993. The epidemiology of heart failure: The Framingham study. *J. Am. Coll. Cardiol.* **22**:6–13.
3. Lloyd-Jones, D.M., et al. 2002. Lifetime risk for developing congestive heart failure: the Framingham Heart Study. *Circulation.* **106**:3068–3072.
4. Molkentin, J.D. 2006. Dichotomy of Ca2+ in the heart: contraction versus intracellular signaling. *J. Clin. Invest.* **116**:623–626.
5. Wu, X., et al. 2006. Local InsP3-dependent perinuclear Ca2+ signaling in cardiac myocyte excitation-transcription coupling. *J. Clin. Invest.* **116**:675–682.

6. Balijepalli, R.C., et al. 2006. Localization of cardiac L-type Ca(2+) channels to a caveolar macromolecular signaling complex is required for beta(2)-adrenergic regulation. *Proc. Natl. Acad. Sci. U. S. A.* **103**:7500–7505.
7. Muth, J.N., Bodi, I., Lewis, W., Varadi, G., and Schwartz, A. 2001. A Ca(2+)-dependent transgenic model of cardiac hypertrophy: a role for protein kinase Calpha. *Circulation.* **103**:140–147.
8. Nakayama, H., et al. 2007. Ca^{2+}- and mitochondrial-dependent cardiomyocyte necrosis as a primary mediator of heart failure. *J. Clin. Invest.* **117**:2431–2444.
9. Wu, X., et al. 2009. Plasma membrane Ca^{2+}-ATPase isoform 4 antagonizes cardiac hypertrophy in association with calcineurin inhibition in rodents. *J. Clin. Invest.* **119**:976–985.
10. Yunker, A.M., and McEnery, M.W. 2003. Low-voltage-activated ("T-Type") calcium channels in review. *J. Bioenerg. Biomembr.* **35**:533–575.
11. Nuss, H.B., and Houser, S.R. 1993. T-type Ca2+ current is expressed in hypertrophied adult feline left ventricular myocytes. *Circ. Res.* **73**:777–782.
12. Martinez, M.L., Heredia, M.P., and Delgado, C. 1999. Expression of T-type Ca(2+) channels in ventricular cells from hypertrophied rat hearts. *J. Mol. Cell. Cardiol.* **31**:1617–1625.
13. Huang, B., Qin, D., Deng, L., Boutjdir, M., and El-Sherif, N. 2000. Reexpression of T-type Ca2+ channel gene and current in post-infarction remodeled rat left ventricle. *Cardiovasc. Res.* **46**:442–449.
14. Bkaily, G., Sculptoreanu, A., Jacques, D., and Jasmin, G. 1997. Increases of T-type Ca2+ current in heart cells of the cardiomyopathic hamster. *Mol. Cell. Biochem.* **176**:199–204.
15. Sen, L., Smith, T.W. 1994. T-type Ca2+ channels are abnormal in genetically determined cardiomyopathic hamster hearts. *Circ. Res.* **75**:149–155.
16. Chiang, C.S., et al. 2009. The Ca(v)3.2 T-type Ca(2+) channel is required for pressure overload-induced cardiac hypertrophy in mice. *Circ. Res.* **104**:522–530.
17. Izumi, T., et al. 2003. Reinduction of T-type calcium channels by endothelin-1 in failing hearts in vivo and in adult rat ventricular myocytes in vitro. *Circulation.* **108**:2530–2535.
18. Lory, P., Bidaud, I., and Chemin, J. 2006. T-type calcium channels in differentiation and proliferation. *Cell Calcium.* **40**:135–146.
19. Massion, P.B., and Balligand, J.L. 2007. Relevance of nitric oxide for myocardial remodeling. *Curr. Heart Fail. Rep.* **4**:18–25.
20. Sanbe, A, et al. 2003. Reengineering inducible cardiac-specific transgenesis with an attenuated myosin heavy chain promoter. *Circ. Res.* **92**:609–616.
21. Jaleel, N., et al. 2008. Ca2+ influx through T- and L-type Ca2+ channels have different effects on myocyte contractility and induce unique cardiac phenotypes. *Circ. Res.* **103**:1109–1119.
22. Mangoni, M.E., et al. 2006. Bradycardia and slowing of the atrioventricular conduction in mice lacking CaV3.1/alpha1G T-type calcium channels. *Circ. Res.* **98**:1422–1430.
23. Calderone, A., Thaik, C.M., Takahashi, N., Chang, D.L., and Colucci, W.S. 1998. Nitric oxide, atrial natriuretic peptide, and cyclic GMP inhibit the growth-promoting effects of norepinephrine in cardiac myocytes and fibroblasts. *J. Clin. Invest.* **101**:812–818.
24. Fiedler, B., et al. 2002. Inhibition of calcineurin-NFAT hypertrophy signaling by cGMP-dependent protein kinase type I in cardiac myocytes. *Proc. Natl. Acad. Sci. U. S. A.* **99**:11363–11368.
25. Gratton, J.P., Bernatchez, P., and Sessa, W.C. 2004. Caveolae and caveolins in the cardiovascular system. *Circ. Res.* **94**:1408–1417.
26. Bers, D.M. 2001. *Excitation-contraction coupling and cardiac contractile force.* 2nd edition. Kluwer Academic Publishers. Dordrecht, The Netherlands. 427 pp.
27. Hullin, R., et al. 2007. Increased expression of the auxiliary beta2-subunit of ventricular L-type Ca2+ channels leads to single-channel activity characteristic of heart failure. *PLoS ONE.* **2**:e292.
28. Freichel, M., et al. 1999. V. Store-operated cation channels in the heart and cells of the cardiovascular system. *Cell Physiol. Biochem.* **9**:270–283.
29. Hunton, D.L., et al. 2002. Capacitative calcium entry contributes to nuclear factor of activated T-cells nuclear translocation and hypertrophy in cardiomyocytes. *J. Biol. Chem.* **277**:14266–14273.
30. Hunton, D.L., Zou, L., Pang, Y., and Marchase, R.B. 2004. Adult rat cardiomyocytes exhibit capacitative calcium entry. *Am. J. Physiol. Heart Circ. Physiol.* **286**:H1124–H1132.
31. Uehara, A., Yasukochi, M., Imanaga, I., Nishi, M., and Takeshima, H. 2002. Store-operated Ca2+ entry uncoupled with ryanodine receptor and junctional membrane complex in heart muscle cells. *Cell Calcium.* **31**:89–96.
32. Nakayama, H., Wilkins, B.J., Bodi, I., and Molkentin, J.D. 2006. Calcineurin-dependent cardiomyopathy is activated by TRPC in the adult mouse heart. *FASEB J.* **20**:1660–1670.
33. Bush, E.W., et al. 2006. Canonical transient receptor potential channels promote cardiomyocyte hypertrophy through activation of calcineurin signaling. *J. Biol. Chem.* **281**:33487–33496.
34. Kuwahara, K., et al. 2006. TRPC6 fulfills a calcineurin signaling circuit during pathologic cardiac remodeling. *J. Clin. Invest.* **116**:3114–3126.
35. Kitchens, S.A., Burch, J., and Creazzo, T.L. 2003. T-type Ca2+ current contribution to Ca2+-induced Ca2+ release in developing myocardium. *J. Mol. Cell. Cardiol.* **35**:515–523.
36. Schmitt, R., Clozel, J.P., Iberg, N., and Buhler, F.R. 1995. Mibefradil prevents neointima formation after vascular injury in rats. Possible role of the blockade of the T-type voltage-operated calcium channel. *Arterioscler. Thromb. Vasc. Biol.* **15**:1161–1165.
37. Kuga, T., Kobayashi, S., Hirakawa, Y., Kanaide, H., and Takeshita, A. 1996. Cell cycle-dependent expression of L- and T-type Ca2+ currents in rat aortic smooth muscle cells in primary culture. *Circ. Res.* **79**:14–19.
38. Wolfe, J.T., Wang, H., Perez-Reyes, E., and Barrett, P.Q. 2002. Stimulation of recombinant Ca(v)3.2, T-type, Ca(2+) channel currents by CaMKIIgamma(C). *J. Physiol.* **538**:343–355.
39. Klockner, U., et al. 1999. Comparison of the Ca2 + currents induced by expression of three cloned alpha1 subunits, alpha1G, alpha1H and alpha1I, of low-voltage-activated T-type Ca2 + channels. *Eur. J. Neurosci.* **11**:4171–4178.
40. Wolfe, J.T., Wang, H., Howard, J., Garrison, J.C., and Barrett, P.Q. 2003. T-type calcium channel regulation by specific G-protein betagamma subunits. *Nature.* **424**:209–213.
41. Zheng, M., et al. 2006. Lysophosphatidylcholine augments Ca(v)3.2 but Not Ca(v)3.1 T-type Ca(2+) channel current expressed in HEK-293 cells. *Pharmacology.* **76**:192–200.
42. Booz, G.W. 2005. Putting the brakes on cardiac hypertrophy: exploiting the NO-cGMP counterregulatory system. *Hypertension.* **45**:341–346.
43. Takimoto, E., et al. 2005. Chronic inhibition of cyclic GMP phosphodiesterase 5A prevents and reverses cardiac hypertrophy. *Nat. Med.* **11**:214–222.
44. Zeng, X., Keyser, B., Li, M., and Sikka, S.C. 2005. T-type (alpha1G) low voltage-activated calcium channel interactions with nitric oxide-cyclic guanosine monophosphate pathway and regulation of calcium homeostasis in human cavernosal cells. *J. Sex Med.* **2**:620–630.
45. Cappola, T.P., et al. 2003. Deficiency of different nitric oxide synthase isoforms activates divergent transcriptional programs in cardiac hypertrophy. *Physiol. Genomics.* **14**:25–34.
46. Ichinose, F., et al. 2004. Pressure overload-induced LV hypertrophy and dysfunction in mice are exacerbated by congenital NOS3 deficiency. *Am. J. Physiol. Heart Circ. Physiol.* **286**:H1070–H1075.
47. Ruetten, H., Dimmeler, S., Gehring, D., Ihling, C., and Zeiher, A.M. 2005. Concentric left ventricular remodeling in endothelial nitric oxide synthase knockout mice by chronic pressure overload. *Cardiovasc. Res.* **66**:444–453.
48. Janssens, S., et al. 2004. Cardiomyocyte-specific overexpression of nitric oxide synthase 3 improves left ventricular performance and reduces compensatory hypertrophy after myocardial infarction. *Circ. Res.* **94**:1256–1262.
49. Takimoto, E., et al. 2005. Oxidant stress from nitric oxide synthase-3 uncoupling stimulates cardiac pathologic remodeling from chronic pressure load. *J. Clin. Invest.* **115**:1221–1231.
50. Kim, D., et al. 2001. Lack of the burst firing of thalamocortical relay neurons and resistance to absence seizures in mice lacking {alpha}1G T-type Ca2+ channels. *Neuron.* **31**:35–45.
51. Xu, J., et al. 2006. Myocyte enhancer factors 2A and 2C induce dilated cardiomyopathy in transgenic mice. *J. Biol. Chem.* **281**:9152–9162.
52. Braz, J.C., et al. 2004. PKC-alpha regulates cardiac contractility and propensity toward heart failure. *Nat. Med.* **10**:248–254.
53. Oka, T., et al. 2006. Cardiac-specific deletion of Gata4 reveals its requirement for hypertrophy, compensation, and myocyte viability. *Circ. Res.* **98**:837–845.
54. Wilkins, B.J., et al. 2004. Calcineurin/NFAT coupling participates in pathological, but not physiological, cardiac hypertrophy. *Circ. Res.* **94**:110–118.